

1
2
3
4
5
6
7
8
9

Micro encapsulation and characterization of Diclosulam in Xanthan Gum based polymeric system for smart delivery of herbicide in crop production

ABSTRACT

Aim: Micro encapsulation of diclosulam herbicide was done in xanthan gum based polymeric system through ionotropic gelation method to formulate a slow-release herbicide to achieve prolonged weed control in irrigated upland ecosystem.

Place and duration of study: The slow-release formulation of diclosulam was synthesized and characterized in the Department of Nano Science & Technology, Tamil Nadu Agricultural University during January to July 2022.

Methodology: Xanthan gum- alginate microsphere system was synthesized with varying concentrations of calcium chloride (CaCl₂) (2, 4 and 6 per cent) to encapsulate diclosulam through ionotropic gelation. The size, entrapment efficiency, pore volume, pore radius, surface area and swelling behavior of microspheres were assessed to achieve higher loading of diclosulam and good stability of microspheres.

Results: The mean diameter of xanthan gum-alginate microsphere was higher with 6 per cent ion gelation bath followed by the concentration of 4 and 2 per cent. Higher entrapment efficiency of diclosulam was achieved with loading of two percent diclosulam in six per cent calcium crosslinked microspheres

Conclusion: Xanthan gum- alginate microsphere system offers both burst release and controlled release of active ingredients. However, controlled release polymeric templates with herbicide will synchronize the release of herbicide with the emergence of weeds in the cropped situations for better weed management.

Keywords: Micro encapsulation, Xanthan gum, Sodium Alginate, Diclosulam, Ion gelation

1. INTRODUCTION

10
11
12
13
14
15
16
17

Herbicides are the second-largest category of plant protection chemical behind insecticides in terms of consumption. The Indian herbicide market had achieved the growth of 12.3 per cent since 2018, compared to the growth of 8.9 per cent for other insecticide and fungicide. The use of herbicides is the efficient strategy to manage weeds in crop production. However, the continuous and indiscriminate use of herbicides cause phytotoxicity in crops, faster

18 degradation due to light, persistence in the soil, and leaching into ground water. Overuse of
19 herbicides affect succeeding crops through the carry over effect in the soil. The development
20 of herbicide-resistant weed species, and shift in weed flora were observed due to the
21 frequent use of herbicides to control weeds [1]. Up to 20 to 25 DAS, pre-emergence
22 herbicides have proven to be very successful, but late-arriving weeds obstruct pegging, pod
23 development, and harvesting [2]. The fate of herbicides in the soil determines the efficiency
24 of herbicidal activity, where rapid conversion of intermediates in the soil making less effective
25 against weeds. In addition, intermediate compounds from the degradation path of herbicides
26 in soil contaminate the groundwater [3]. Diclosulam (2', 6'-dichloro-5-ethoxy-7-fluoro [1,2,4]
27 triazolo[1,5-c] pyrimidine-2-sulfonamide) is a low volume herbicide belonging to sulfonamide
28 family. Diclosulam interfere with Aceto Hydroxy Acid Synthase (AHAS), a key enzyme
29 involved in the synthesis of branched-chain amino acids such as leucine, isoleucine and
30 valine in plants, thus affecting protein synthesis and cell division that leads to death of
31 targeted weeds. Diclosulam is recommended as pre-emergence herbicide (soybean,
32 groundnut, sorghum, potato, maize, wheat, barley and oats), applied at 1 to 3 days after
33 sowing with the optimum dose of 20 g a.i. ha⁻¹ for groundnut [2]. Phytotoxicity symptoms
34 such as yellowing of leaves are reported in groundnut with the application of diclosulam.
35 Similarly, pre-emergence application of diclosulam controls weeds up to 40 days of sowing in
36 groundnut which warrants either hand weeding and post emergence application of herbicides
37 to maintain weed free situation to prevent economic yield loss. Diclosulam binds with soil that
38 leads to less mobility and leaching in soils causing less herbicidal activity. Hence, the
39 research was proposed to design diclosulam systems for releasing active molecules at
40 regulated manner to maintain the concentration of herbicide in soil to cause herbicidal action.

41

42 Encapsulation with natural polymers is the best strategy to improve weed control efficiency of
43 herbicides and reduce herbicide adsorption in the soil. Microsphere encapsulation of
44 agrochemicals in pectin based polymeric system was used for the smart release of
45 herbicides [4]. Diverse properties of natural polymers were preferred for encapsulation of
46 herbicides over synthetic materials due to non-toxicity in nature, abundance availability and
47 the cost [5]. Xanthan gum and alginate are natural polymers, explored as a carrier for
48 encapsulation of plant protection chemicals and microbes. Xanthan gum is a microbial extra
49 cellular polysaccharide produced by Gram negative aerobic bacteria *Xanthomonas*
50 *campestris* [6]. Xanthan gum is biocompatible in nature, bio adhesive, biodegradable, non-
51 toxic and low cost which makes suitable candidate for the encapsulation of agrochemicals
52 [7]. Biofilms, hydrogels, micro particles and nanoparticle of xanthan gum and xanthan gum
53 based composites are widely used for designing controlled release systems [8]. Xanthan

54 gum acts as emulsifier and thickening agent besides its good water-control properties and
55 pseudoplastic behavior, where xanthan gum at lower concentrations readily form high
56 viscous solution exhibiting pseudoplasticity [9]. Sodium alginate is an anionic polysaccharide
57 derived from sea algae (Phaeophyceae) that contain 30–60 per cent of alginic acid. Sodium
58 salt of alginic acid is a linear polymer made up of residues of 1, 4-linked D-mannuronic acid
59 and D-gluronic acid. Sodium alginate nanoparticles are also explored for designing pesticide
60 delivery systems due to its biodegradability, biocompatibility, and low toxicity in nature.
61 Therefore, the present study focuses on designing xanthan gum and sodium alginate based
62 polymeric system for the delivery of diclosulam for improving weed control efficiency

63 **2. MATERIAL AND METHODS**

64 **2.1. Materials**

65 Sodium alginate (HiMedia: Cat No. RM7494) was purchased from HiMedia (Mumbai, India)
66 while methanol (Merck: Cat. No. 494291) was obtained from Sigma Aldrich (Mumbai, India).
67 IAMPURE Ingredients (Chennai, India) supplied xanthan gum. Calcium chloride anhydrous
68 (Avra: Cat No. ASC2461)) was purchased from Avra Synthesis Private Limited. (Hyderabad,
69 India), Phosphate buffer was procured from Molychem (Mumbai, India), Diclosulam herbicide
70 (84% WDG) and ethanol were purchased locally. None of the chemicals was further purified
71 before being employed in the study.

72 **2.2. Methods**

73 **2.2.1. Encapsulation of diclosulam in Xanthan gum - Alginate microspheres**

74 Xanthan gum (XG) – Sodium alginate (SA) microspheres were prepared based on the
75 earlier protocol [10] with some modifications through ionotropic gelation method. A
76 homogeneous solution of xanthan gum and sodium alginate were prepared by dissolving in
77 water using a reflux condenser at 45°C. The ratio of sodium alginate to xanthan gum was
78 kept as 1:0.67 for the preparation of microspheres. The XG/SA mixture was dropped to ion
79 gelation bath of calcium chloride (2, 4 and 6 per cent) to obtain microspheres. The distance
80 between the delivery point of syringe and ionic solution was maintained at 7cm, while flow
81 rate of polymer mixture was kept at 16 drops minute⁻¹. Microspheres were cured in the
82 gelation bath for 45 minutes in the room temperature. Subsequently, microspheres were
83 washed with deionized water to remove non-cross-linked cations over the surface of the
84 beads. Beads were dried at room temperature for 48h until obtaining uniform weight of
85 beads. Diclosulam was homogenized in the polymer matrix before dropping into gelation bath
86 to facilitate the encapsulation of diclosulam in the polymeric systems

87 **2.2.2. Entrapment efficiency of Diclosulam in Microspheres**

88 Encapsulation efficiency represents the amount of active ingredient encapsulated in matrix
89 complexes of xanthan gum-alginate polymeric systems. Herbicide loaded beads of varying
90 concentrations were analyzed individually using UV-Vis spectrophotometer (Analytik Jena,
91 Specord 210 Plus). Diclosulam (84 per cent WDG) was prepared to 10 ppm using 0.067 M
92 phosphate buffer (6.8 pH) for assessing the wavelength of maximum absorption through
93 scanning with a wavelength of 200 to 800 nm in UV Vis spectroscopy. The known
94 concentrations of diclosulam (5, 10, 15, 20, 25 and 30 ppm) standards were used to find OD
95 values in UV Vis spectroscopy for obtaining standard curve. Similarly, microspheres (20 mg)
96 containing diclosulam were dissolved in 10 ml of 0.067 M phosphate buffer (6.8 pH) for 4h
97 complete dissolution of microspheres. Aliquot was filtered through membrane filter (0.22µm)
98 to reduce the residual interaction and analyzed at $\lambda_{max} = 251$ nm using a
99 spectrophotometer. Diclosulam entrapment efficiency was calculated using the following
100 formula

$$101 \text{ Encapsulation Efficiency (\%)} = \frac{\text{Actual herbicide content}}{\text{Theoretical herbicide content}} \times 100$$

102 **2.2.3. Swelling behavior and water uptake of microspheres**

103 The swelling property and water uptake of diclosulam-loaded xanthan gum – alginate
104 microspheres were assessed in terms of change in mass and diameter with function of time.
105 Measurements of the initial diameter and mass of dried microspheres were made before
106 beads were soaked for two hours at room temperature in phosphate buffer (6.8 pH). The
107 microspheres were retrieved from phosphate buffer in a regular intervals to assess mass and
108 diameter at time 't'. The percent of water uptake and swelling per cent were calculated using
109 following equations

$$110 \text{ Percent Swelling} = \frac{\text{Diameter of microsphere at time "t" - Initial diameter of microsphere}}{\text{Initial diameter of microsphere}} \times 100$$

$$111 \text{ Water uptake} = \frac{\text{Weight of microsphere at time "t" - Initial weight of microsphere}}{\text{Initial weight of microsphere}} \times 100$$

112 **2.2.4. Characterization of diclosulam loaded xanthan gum -alginate microspheres**

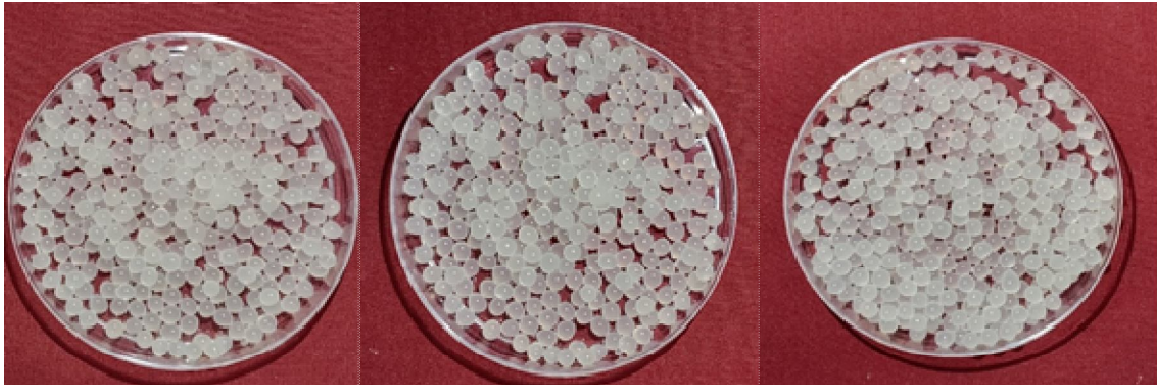
113 Diclosulam loaded xanthan gum – alginate microspheres were examined under digital
114 optical fluorescent microscope (ProgRes C5 indi) at 5x magnification to determine the size of
115 microsphere. The surface topography of microspheres was assessed using scanning
116 electron microscope (Quanta 250, FEI, Czech Republic). Electron microscopy images were
117 obtained by mounting the microsphere on carbon stub at an acceleration voltage of 10kV
118 with chamber pressure of 1.0mm Hg. Fourier Transformed Infra-Red spectra of xanthan
119 gum, sodium alginate, diclosulam, xanthan gum – alginate microsphere and diclosulam
120 loaded xanthan gum – alginate microsphere was recorded using JASCO –FTIR-6800.

121 Attenuated total reflection (ATR) mode was used at wavenumber regime of 4000 to 400 cm^{-1}
122 with 4 cm^{-1} resolution and 32 scans. The pore size, pore radius and surface area of
123 microspheres were assessed using Brunner –Emmet-Teller (Quantachrome NOVAtouch
124 NT2LX-1). The microspheres were degassed at 100°C for 3h to remove moisture and
125 subjected to the adsorption of nitrogen gas at series of pressure points (0 to 800 torr).

126 **3. RESULTS AND DISCUSSION**

127 Encapsulation of diclosulam in xanthan gum –sodium alginate polymeric microcapsules or
128 microspheres was carried out through ionic gelation technique. The concentration of ion
129 gelation bath affected the size and behaviour of xanthan gum –sodium alginate
130 microspheres. Fresh and dried xanthan gum - sodium alginate microsphere without loading
131 diclosulam cross-linked with various concentration of ion gelation bath (calcium chloride) are
132 illustrated in Fig 1a, 1b, 1c and 2a, 2b and 2c. The microspheres were completely spherical
133 in nature irrespective of ion gelation bath concentrations. Gelation occurs through ionic
134 bonding between divalent cations in the gelation bath and carboxyl group of guluronic acids
135 in sodium alginate and mannose units in xanthan gum. Gelation process results in the
136 formation of three-dimensional structures, which further are stabilized through the exchange
137 of sodium ions in the polymer matrix with divalent calcium ions in the gelation bath. The rate
138 of divalent cations in gelation bath determines the sphericity of microspheres. The regain of
139 spherical shape of polymer beads in the ion gelation bath occurs when the viscous force of
140 polymers overcome the drag force of ion gelation bath [10]. Hence, the concentration of
141 xanthan gum and sodium alginate used in the study creates viscous force to regain the
142 spherical shape of beads through overcoming drag forces of ion gelation bath. Chloride ions
143 interact with uronic acid of sodium alginate to form calcium alginate xanthan layer externally
144 over the bead exchanging sodium ions. The digital fluorescence microscopic image of
145 calcium chloride cross-linked xanthan gum-alginate microspheres shows a uniform
146 undulation (black color) from periphery to center of the bead, which was cross-linked with two
147 per cent of ion gelation bath (fig.3a). On the other hand, thick outer shell and smooth inner
148 core were observed in beads cross-linked with, six per cent ion gelation bath (fig.3c). The
149 wall materials surrounding the core molecules (herbicide) attribute to the greater
150 improvement of physical and chemical stability and control the delivery of core materials [11,
151 12]. Matrix polymeric type delivery system (microspheres) offers the controlled release of
152 core material through equidistant matrix erosion after a burst release at initial phase of
153 delivery. Hence, the effects of calcium chloride concentrations (ionic cross linker) were
154 observed in the digital images of fluorescent microscope. Higher rate of divalent ions
155 complexes readily with peripheral layer of polymer matrix, thus resisting further penetration of

156 divalent calcium into center of beads resulting in poor crosslinking. Lower concentration of
157 divalent ions in the gelation bath allows the movement of cations into beads completely to
158 achieve higher crosslinking. The intensity of black coloration in the images indicates the
159 intensity of calcium ions, where beads cross-linked with six per cent calcium chloride results
160 in the thick black peripheral layer over the bead representing higher concentration of calcium
161 ions and vice versa.



[1a]

[1b]

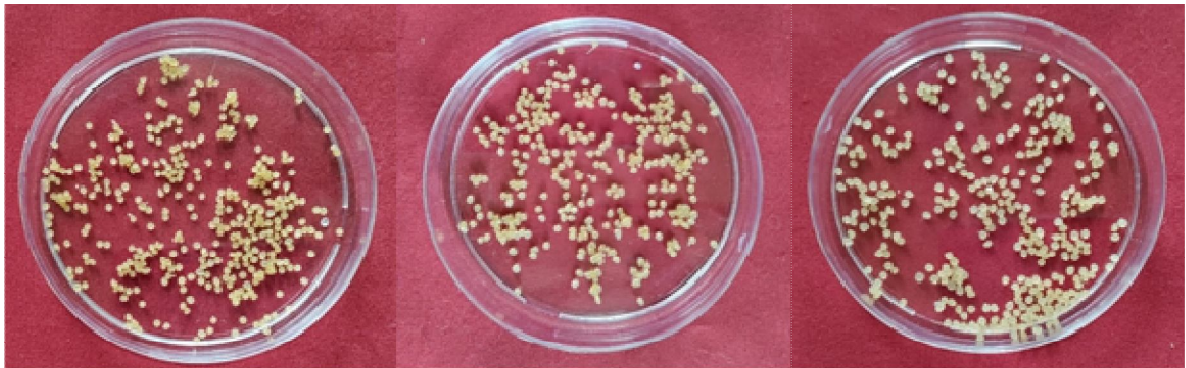
[1c]

162

163

164

Fig 1: Fresh Xanthan gum alginate microspheres: [1a]: 2% calcium chloride cross linked; [1b]: 4% calcium chloride cross linked; [1c]: 6% calcium chloride cross linked



[2a]

[2b]

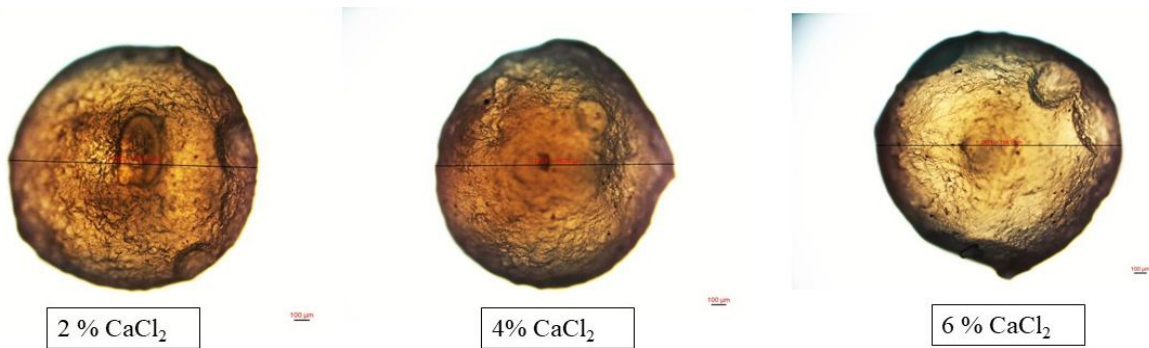
[2c]

165

166

167

Fig 2: Dried Xanthan gum alginate microspheres: [2a]: 2% calcium chloride cross linked; [2b]: 4% calcium chloride cross linked; [2c]: 6% calcium chloride cross linked.



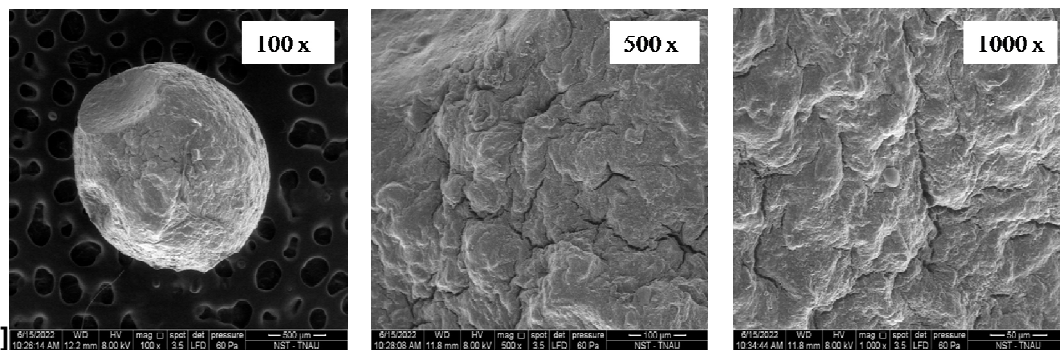
168
169
170

Fig 3: Digital optical fluorescent microscopic image of two, four and six percent Calcium chloride cross linked Xanthan gum – Alginate microsphere

171 A uniform influx of calcium ions with efflux of water and sodium ions occurs at low
172 concentration of ion gelation bath, whereas maximum cross-linking forms with higher
173 concentration of calcium chloride at outer layer of polymer matrix (bead) that becomes
174 hardened and prevents the further influx of calcium ions for cross linking, thus forming a
175 smooth inner core.

176 Scanning electron microscopic images of xanthan gum sodium alginate microspheres are
177 illustrated in fig.4., which substantiate the above statement with a gradual decline in cracks or
178 pinholes with increasing concentration of calcium ions in ion gelation bath. The shape and
179 average diameter of xanthan gum-alginate microspheres are tabulated (Table1), which
180 indicates the mean diameter of microsphere increases with increasing concentration of
181 calcium chloride. Calcium ion influx, force efflux of water molecules and makes the
182 microspheres to downsize resulting in smaller bead size at lower concentration of ion
183 gelation bath. The mean diameter of beads, which were cross-linked, with concentration of
184 six per cent calcium chloride resulted in larger bead size (2.00 mm) compared to beads (1.61
185 mm) cross-linked with two per cent concentration of calcium chloride.

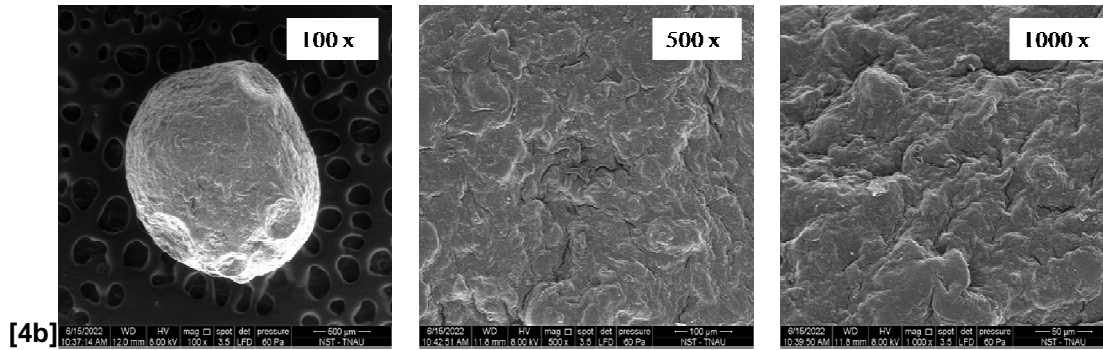
186



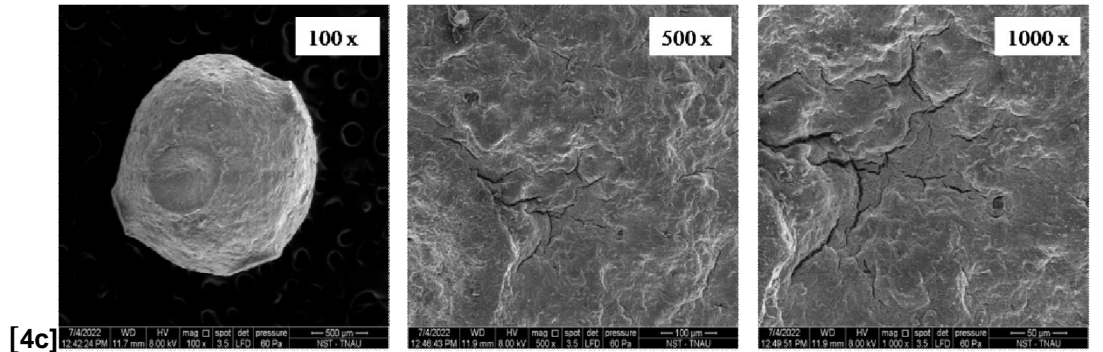
187

[4a]

188



189



190 **Fig 4: SEM micrographs of Calcium chloride cross linked Xanthan gum-alginate**
 191 **microsphere; [a]: 2% CaCl₂ Cross linked; [b]: 4% CaCl₂ Cross linked; [c]: 6% CaCl₂**
 192 **Cross linked.**

193 **Table 1: Effect of various concentration of calcium chloride on mean diameter and**
 194 **shape of xanthan gum alginate microspheres**

Concentration of Calcium chloride (%)	Diameter (mm)	Remarks
2 per cent	1.61	Beads were round and spherical
4 per cent	1.63	Beads were round and spherical
6 per cent	2.00	Beads were oval

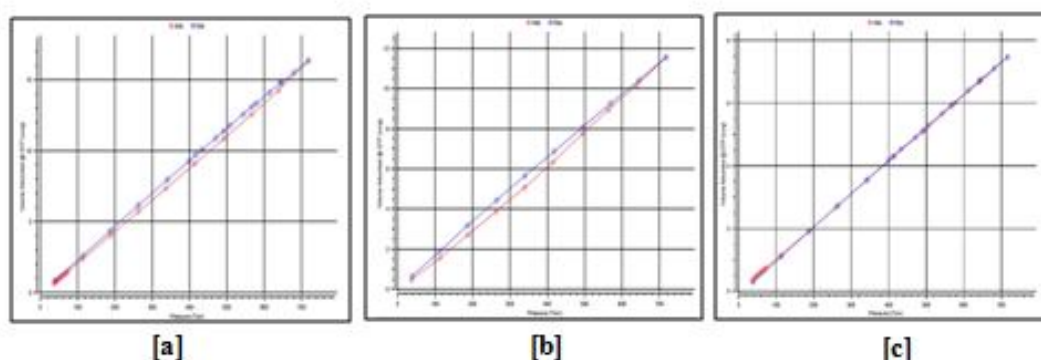
195 Pore volume and surface area governs the water uptake and dissolution of active molecules
 196 loaded in the polymeric matrix system. Cross linking of polymers with different concentration
 197 of ionic solution influence the surface area and pore volume of microspheres (Table 2). The
 198 surface area (1.92 m² g⁻¹) and pore radius (2.94 nm) of microspheres were higher with
 199 crosslinking of two per cent calcium chloride, while beads complexed with six per cent
 200 calcium chloride have less surface area (1.05 m² g⁻¹) and pore radius (2.44 nm)

201 Thus, ionic solution concentration is inversely proportional to pore volume and surface area.
 202 This implies that, a greater number of functional groups in polymers reacted at increasing
 203 concentration of ionic solution resulting in increased bead size. Hence, downsizing of beads
 204 with lower concentration of cross linkers proved with higher surface area, while uniform

205 crosslinking throughout the polymer matrix in lower concentration of calcium chloride
 206 promotes higher pore radius. The type I isotherm (fig.5) of calcium chloride cross-linked
 207 beads exhibits monolayer adsorption of gaseous molecules confirming the micro porous
 208 nature of polymeric beads. Hence, the pore volume and surface area are foremost
 209 parameter determining the release of core materials into the medium.

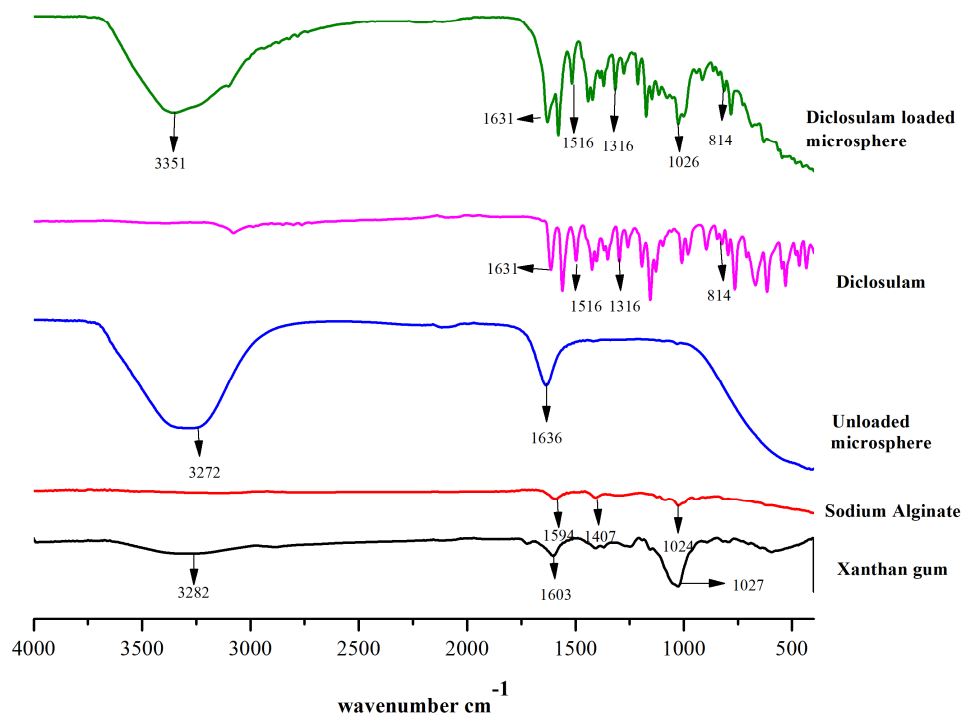
210 **Table 2: Effect of various concentration of calcium chloride on pore volume, pore**
 211 **radius and surface area of xanthan gum alginate microsphere.**

Treatments	Pore volume (cc/g)	Pore radius (nm)	Surface area (m ² /g)
Calcium chloride 2%	0.024	2.94	1.92
Calcium chloride 4%	0.017	2.94	1.45
Calcium chloride 6%	0.011	2.44	1.05



212 **Fig 5: Effect of Calcium chloride concentration on absolute isotherms of xanthan gum-**
 213 **alginate microsphere.**

215 Further, diclosulam (hydrophobic moiety) was encapsulated in xanthan gum alginate
 216 microspheres. The gelation of polymeric molecules entraps diclosulam simultaneously
 217 through gelation with calcium divalent ions. Thus, ionic bond formed between calcium ions
 218 and, carboxyl and hydroxyl groups of polymers favoring the formation of “egg box” complex
 219 [13-16]. The three-dimensional structures get stabilized through exchanging sodium ions
 220 with calcium ions in the polymeric system, provided maximum stability by minimizing internal
 221 entropy[17], represented in the infra-red spectra of diclosulam loaded polymeric system (fig
 222 6) forming strong bridging complex with disappearance of 1407cm⁻¹peak corresponding to
 223 OH bending of carboxylic acid.

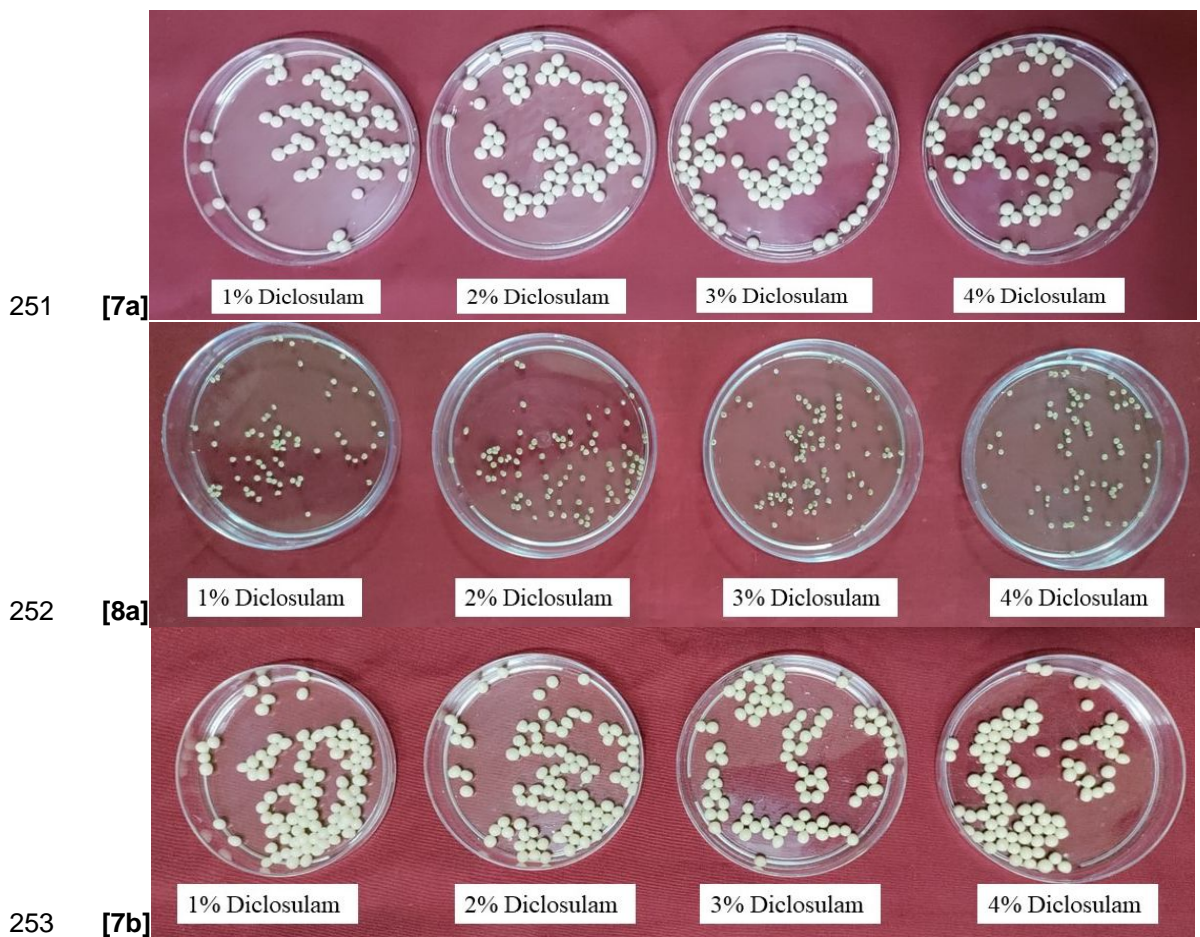


224

225 **Fig 6: FTIR spectrum of xanthan gum, sodium alginate, xanthan gum – alginate**
 226 **microsphere, diclosulam and diclosulam loaded xanthan gum – alginate microsphere**

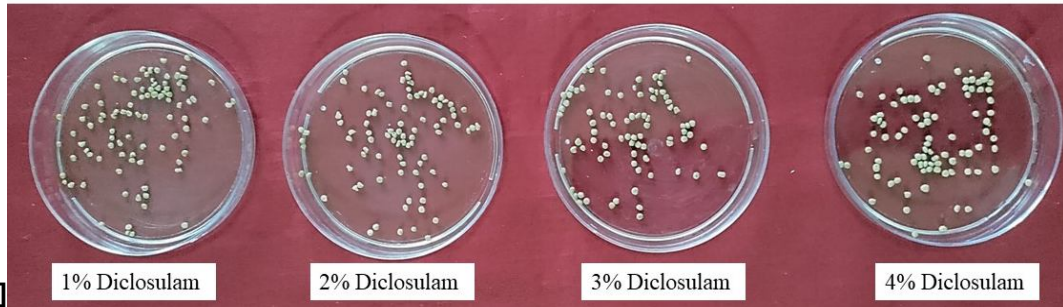
227 The calcium ions offer instantaneous formation of bridging complex between carboxyl
 228 groups of xanthan gum – sodium alginate polymeric system, indicates the formation of
 229 partial covalent bond with decrease or disappearance of COO^- stretching peak at 1024 cm^{-1}
 230 of sodium alginate and shift to higher wavenumber 1631 cm^{-1} confirming the complexation
 231 process in cross-linked polymeric system [18-20]. The intermolecular hydrogen bonding
 232 formed between sodium alginate and xanthan gum was more prominent with an increased
 233 intensity peak at 3272 cm^{-1} in the cross-linked polymeric system [21, 22]. The physical
 234 adsorption of diclosulam to xanthan gum-alginate microspheres were confirmed through the
 235 presence of characteristic vibrational peaks of 1578, 1516, 850 to 550 corresponding to
 236 crystalline nature and C-Cl stretching of halo compounds in diclosulam loaded polymeric
 237 system (Fig 6). Different concentrations of diclosulam were loaded in xanthan gum alginate
 238 microspheres. The fresh and dry beads of diclosulam loaded xanthan gum alginate
 239 microspheres were shown in fig 7&8 respectively. The mean diameter of diclosulam loaded
 240 xanthan gum-alginate microsphere increases with increasing concentration of diclosulam
 241 (Table 3). Bead diameters of diclosulam-entrapped microspheres were increased with

242 concentration of diclosulam up to three per cent, whereas microspheres with four per cent of
243 diclosulam resulted in lower size irrespective of concentration of ion gelation bath. Mean size
244 of microspheres with one percent diclosulam was 2.12 mm, whereas the average diameter
245 of beads with three per cent diclosulam was 2.30 mm. The size of microspheres with loading
246 of diclosulam with four percent concentration was 2.10 mm, indicating the lesser size of
247 beads with higher concentration of diclosulam beyond three per cent. Mass of diclosulam
248 loaded microspheres increases gradually with increasing concentration of diclosulam.
249 However, the discrepancy in mass and diameter of microspheres loaded with four per cent
250 diclosulam might be due to the increased specific gravity of polymer solution.



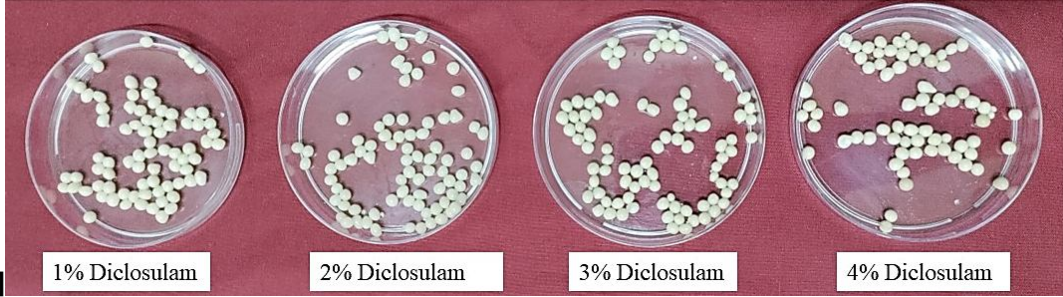
254

[8b]



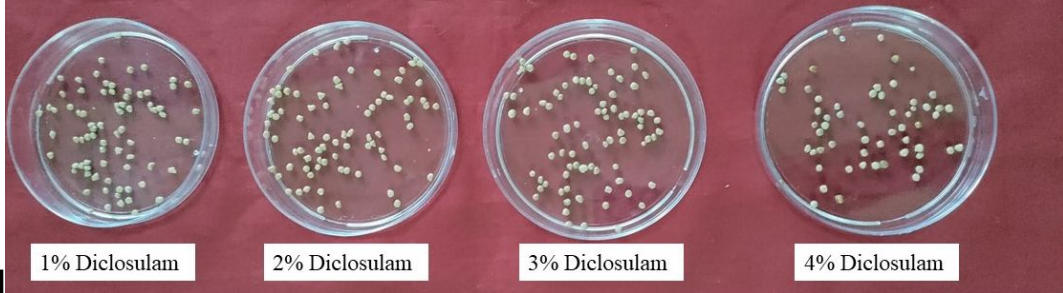
255

[7c]



256

[8c]

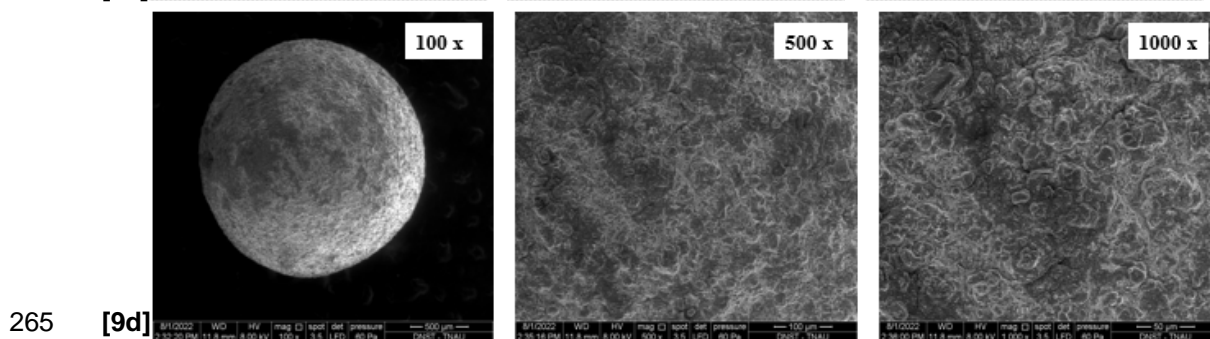
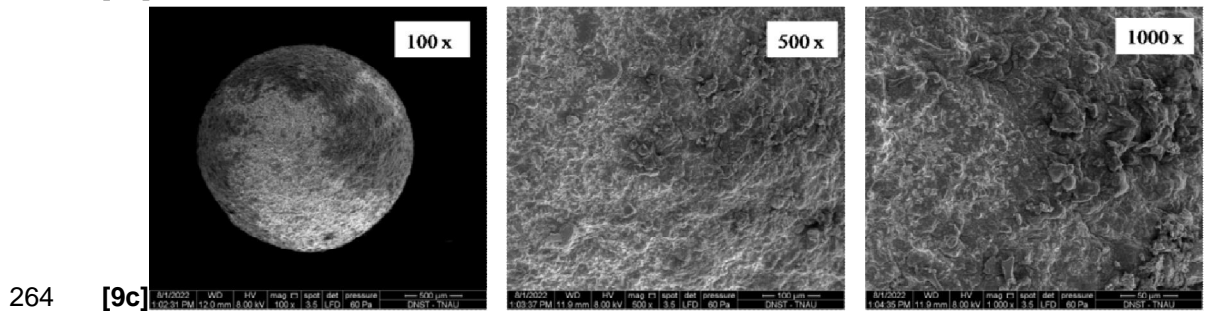
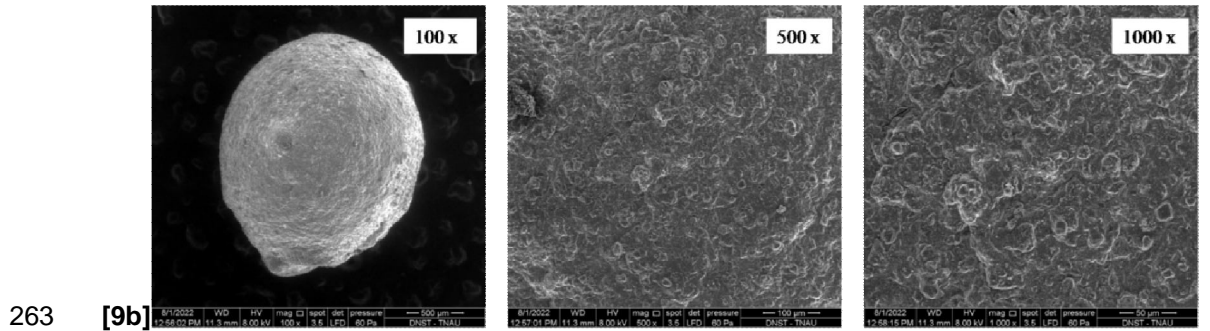
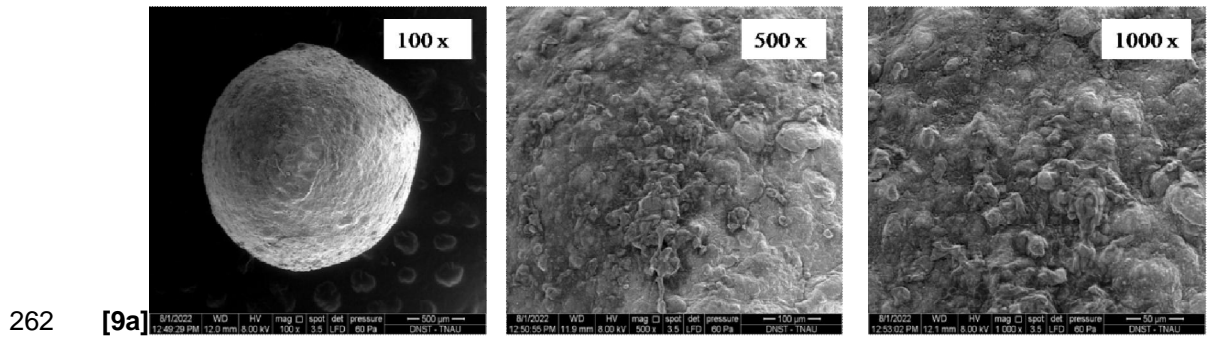


257 **Fig 7&8: Diclosulam loaded Xanthan gum-Alginate fresh and dry microsphere**
 258 **respectively; [7a&8a]: 2% CaCl₂ crosslinked; [7b&8b]: 4% CaCl₂ Crosslinked; [7c&8c]:**
 259 **6% CaCl₂ crosslinked**

260 **Table 3: Effect of calcium chloride and diclosulam concentrations on mean size and**
 261 **shape of xanthan gum alginate microspheres**

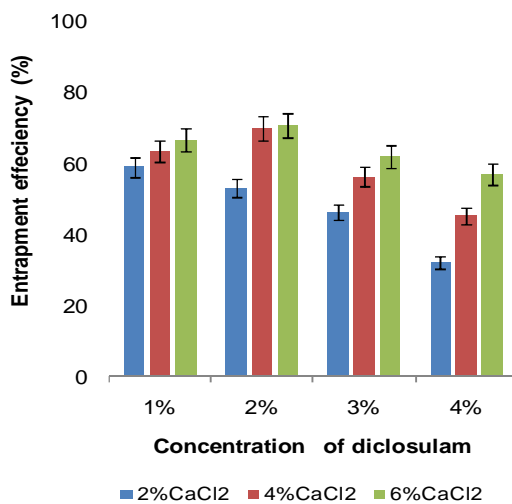
Calcium chloride	Diclosulam	Diameter (mm)	Remarks
2 percent	1 percent	1.99	Beads were round and spherical
	2 percent	2.16	Beads were round and spherical
	3 percent	2.26	Beads were round
	4 percent	2.02	Initially beads were round and turns oval upon increasing the gelation time
4 percent	1 percent	2.14	Beads were round and spherical
	2 percent	2.26	Beads were round and spherical
	3 percent	2.28	Beads were round
	4 percent	2.16	Initially beads were round and turns oval upon increasing the gelation time

6 percent	1 percent	2.25	Beads were round and spherical
	2 percent	2.27	Beads were round and spherical
	3 percent	2.38	Beads were round
	4 percent	2.13	Initially beads were round and turns oval upon increasing the gelation time



266 **Fig 9: SEM micrographs of diclosulam loaded in two percent calcium chloride**
267 **crosslinked xanthan gum alginate microsphere; [a] 1% Diclosulam loaded; [b]: 2%**
268 **Diclosulam loaded; [c]: 3% diclosulam loaded; [d]: 4% diclosulam loaded.**

269 Scanning electron microscopic images of diclosulam loaded polymeric system revealed that,
270 appearance of fringes of xanthan gum – alginate microspheres and exhibition of protrusions
271 over the surface of microspheres forming an undulated surface which signifies the presence
272 of particulate matter. The intensity of particulate matter increases with increasing
273 concentration of diclosulam (fig 9) loaded in the polymeric system. A comparison of
274 entrapment efficiency of various concentration of diclosulam loaded in xanthan gum –
275 alginate microsphere was shown in fig 10. The entrapment efficiency of diclosulam
276 decreases with increasing concentration of diclosulam in xanthan gum alginate
277 microspheres. The higher concentration of diclosulam increases the polymer to drug ratio,
278 thereby it reaches saturation and declines the entrapment efficiency. Higher entrapment
279 efficiency (69.6 and 70.3 per cent) of diclosulam was noticed in six percent and four percent
280 calcium cross linked microspheres loaded with two percent diclosulam followed by two per
281 cent calcium cross linked microspheres with one per cent diclosulam with an entrapment
282 efficiency of 58.6 per cent. The lowest entrapment efficiency was observed in microspheres
283 with loading of diclosulam @ four per cent, might be due to efflux of diclosulam molecules out
284 of polymeric system to achieve equilibrium diffusion coefficient with surrounding ion gelation
285 bath. Conversely, [23, 24] reported that, entrapment efficiency decreases with increasing
286 concentration of crosslinkers.

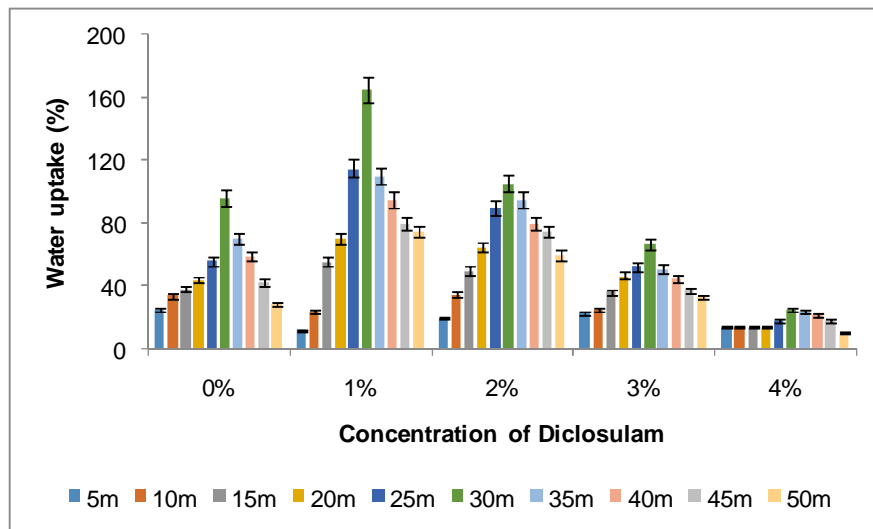


287

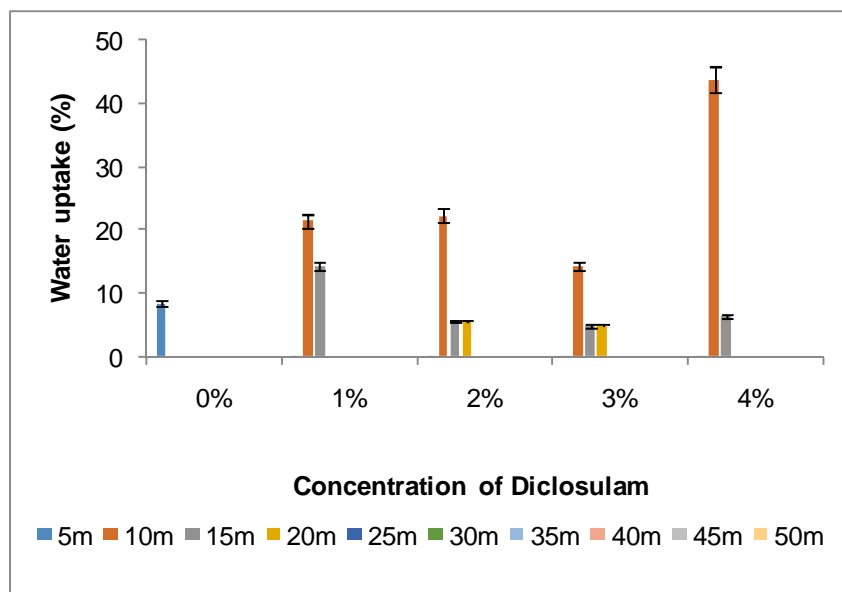
288 **Fig 10: Effect of calcium chloride and diclosulam concentration on entrapment**
289 **efficiency of diclosulam in Xanthan gum alginate microsphere**

290 Water uptake in the polymeric systems determines release kinetics of entrapped functional
291 materials. The effect of various concentrations of calcium chloride on water uptake of
292 diclosulam-loaded microspheres was shown in fig.11. The percent of water uptake increases
293 with time in microspheres with irrespective cross linker concentration. The higher water
294 uptake was observed at 35th minute in microspheres cross-linked with two per cent
295 concentration of calcium chloride followed by four per cent. However, microspheres formed
296 with six per cent calcium chloride get dissipated in water medium within 10 minutes of
297 incubation.

298



299



300

301 **Fig 11: Effect of different concentration of calcium chloride on water uptake of**
 302 **diclosulam loaded (1%, 2%, 3% & 4%) and unloaded xanthan gum-alginate**
 303 **microsphere; [a]: 2% CaCl₂ crosslinked; [b]:4% CaCl₂ crosslinked; [c]: 6% CaCl₂**
 304 **crosslinked;**

305 Lesser water uptake in microspheres cross-linked with six per cent of calcium chloride was
 306 due to high degree of cross-linking over the surface. Swelling studies of microspheres
 307 indicated that beads cross-linked with lesser concentration of calcium chloride (2 and 4 per
 308 cent) absorbs water and reached maximum uptake of water during 30 to 35 minutes of
 309 incubation, while microspheres with six per cent attained maximum water uptake with 10
 310 minutes of incubation. Slower water influx was observed in the polymeric microsphere matrix
 311 formed with lesser concentration of calcium during the initial phase of incubation and
 312 reaches saturation with completely disintegrated microsphere polymer. Microspheres cross
 313 linked with higher concentration of calcium attain saturation rapidly and dissolves with burst
 314 release of functional molecule through poorly crosslinked core region[25].

315 **4. CONCLUSION**

316 This study revealed that calcium mediated ionotropic gelation of xanthan gum-alginate
 317 composite resulted in spherical and stable beads possessing ability for the sustained release
 318 of diclosulam. The mean diameter of xanthan gum microsphere increased from 1.61mm to
 319 2.00 mm with increasing concentration of calcium ions in gelation bath. The entrapment
 320 efficiency of diclosulam @ two percent was higher with crosslinking of 4 and 6 per cent
 321 calcium gelation bath, however, microspheres cross-linked with higher concentration
 322 achieved burst release of diclosulam due to complete dissolution in 10 minutes of incubation

323 in water medium. The microspheres with lower cross linker concentration offers controlled
324 release of active molecules, which proved from the water uptake studies. Burst releases of
325 mechanism of microspheres are not for the delivery of diclosulam herbicide due to localized
326 release of diclosulam from microspheres that induces phytotoxicity. Microspheres cross-
327 linked with two and four per cent calcium chloride offers controlled release of diclosulam,
328 which synchronize with crop growth duration, will not cause phytotoxicity in crops and
329 achieve prolonged weed control.

330 **ACKNOWLEDGEMENTS**

331 All authors acknowledged the Department of Nano Science & Technology and Department of
332 Agronomy for availing the infrastructure to carry out the experiment in Tamil Nadu
333 Agricultural University.

334 **COMPETING INTERESTS**

335 Authors have declared that no competing interest exists.

336

337 **REFERENCES**

338

- 339 1. Sunitha, N. and D.L. Kalyani, *Weed management in maize (Zea mays L.)-a review*.
340 *Agricultural Reviews*, 2012. **33**(1).
- 341 2. Kumar, B.N., et al., *Weed management in groundnut with new herbicide molecules*.
342 *Indian Journal of Weed Science*, 2019. **51**(3): p. 306-307.
- 343 3. Aktar, W., D. Sengupta, and A. Chowdhury, *Impact of pesticides use in agriculture:*
344 *their benefits and hazards*. *Interdisciplinary toxicology*, 2009. **2**(1): p. 1-12.
- 345 4. Pavithran, P., et al., *Synthesis and Characterization of Pectin Beads for the Smart*
346 *Delivery of Agrochemicals*. 2021.
- 347 5. Pandey, S. and S.B. Mishra, *Graft copolymerization of ethylacrylate onto xanthan*
348 *gum, using potassium peroxydisulfate as an initiator*. *International journal of*
349 *biological macromolecules*, 2011. **49**(4): p. 527-535.
- 350 6. Petri, D.F., *Xanthan gum: A versatile biopolymer for biomedical and technological*
351 *applications*. *Journal of Applied Polymer Science*, 2015. **132**(23).
- 352 7. Rajeswari, K.R., et al., *Development and characterization of valsartan loaded*
353 *hydrogel beads*. *Der Pharmacia Lettre*, 2012. **4**: p. 1044-1053.
- 354 8. Cortes, H., et al., *Xanthan gum in drug release*. *Cellular and Molecular Biology*,
355 2020. **66**(4): p. 199-207.
- 356 9. Lopes, B.d.M., et al., *Xanthan gum: properties, production conditions, quality and*
357 *economic perspective*. *J. Food Nutr. Res*, 2015. **54**(3): p. 185-194.
- 358 10. Pongjanyakul, T. and S. Puttipatkhachorn, *Xanthan–alginate composite gel beads:*
359 *molecular interaction and in vitro characterization*. *International Journal of*
360 *Pharmaceutics*, 2007. **331**(1): p. 61-71.
- 361 11. Bannikova, A., et al., *Microencapsulation of fish oil with alginate: In-vitro evaluation*
362 *and controlled release*. *LWT*, 2018. **90**: p. 310-315.
- 363 12. Menin, A., et al., *Effects of microencapsulation by ionic gelation on the oxidative*
364 *stability of flaxseed oil*. *Food Chemistry*, 2018. **269**: p. 293-299.
- 365 13. Banerjee, A., D. Nayak, and S. Lahiri, *A new method of synthesis of iron doped*
366 *calcium alginate beads and determination of iron content by radiometric method*.
367 *Biochemical Engineering Journal*, 2007. **33**(3): p. 260-262.

- 368 14. Chandy, T., D.L. Mooradian, and G.H. Rao, *Evaluation of modified*
369 *alginate-chitosan-polyethylene glycol microcapsules for cell encapsulation*. Artificial
370 organs, 1999. **23**(10): p. 894-903.
- 371 15. Leick, S., et al., *Deformation of liquid-filled calcium alginate capsules in a spinning*
372 *drop apparatus*. Physical Chemistry Chemical Physics, 2010. **12**(12): p. 2950-2958.
- 373 16. Martinsen, A., I. Storrø, and G. Skjærk-Bræk, *Alginate as immobilization material: III.*
374 *Diffusional properties*. Biotechnology and bioengineering, 1992. **39**(2): p. 186-194.
- 375 17. Nunes, R. and E. Rotstein, *Thermodynamics of the water-foodstuff equilibrium*.
376 Drying Technology, 1991. **9**(1): p. 113-137.
- 377 18. Nakanishi, K. and P.H. Solomon, *Infrared absorption spectroscopy*. 1977: Holden-
378 day.
- 379 19. Wanchoo, R. and P. Sharma, *Viscometric study on the compatibility of some water-*
380 *soluble polymer-polymer mixtures*. European Polymer Journal, 2003. **39**(7): p.
381 1481-1490.
- 382 20. Tang, C.Y., Z. Huang, and H.C. Allen, *Binding of Mg²⁺ and Ca²⁺ to palmitic acid*
383 *and deprotonation of the COOH headgroup studied by vibrational sum frequency*
384 *generation spectroscopy*. The Journal of Physical Chemistry B, 2010. **114**(51): p.
385 17068-17076.
- 386 21. Puttipatkhachorn, S., T. Pongjanyakul, and A. Priprem, *Molecular interaction in*
387 *alginate beads reinforced with sodium starch glycolate or magnesium aluminum*
388 *silicate, and their physical characteristics*. International journal of pharmaceutics,
389 2005. **293**(1-2): p. 51-62.
- 390 22. Sartori, C., et al., *Determination of the cation content of alginate thin films by FTi. r.*
391 *spectroscopy*. Polymer, 1997. **38**(1): p. 43-51.
- 392 23. Singh, B.N. and K.H. Kim, *Effects of divalent cations on drug encapsulation*
393 *efficiency of deacylated gellan gum*. Journal of microencapsulation, 2005. **22**(7): p.
394 761-771.
- 395 24. Maiti, S., et al., *Tailoring of locust bean gum and development of hydrogel beads for*
396 *controlled oral delivery of glipizide*. Drug Delivery, 2010. **17**(5): p. 288-300.
- 397 25. Sugawara, S., T. Imai, and M. Otagiri, *The controlled release of prednisolone using*
398 *alginate gel*. Pharmaceutical research, 1994. **11**(2): p. 272-277.

